

Phase transitions in the condition-number distribution of Gaussian random matrices

Isaac Pérez Castillo,¹ Eytan Katzav,² and Pierpaolo Vivo^{3,*}

¹*Departamento de Sistemas Complejos, Instituto de Física, Universidad Nacional Autónoma de México, México D.F. C.P. 04510, México*

²*Racah Institute of Physics, The Hebrew University, Jerusalem 91904, Israel*

³*Department of Mathematics, King's College London, Strand, London WC2R 2LS, United Kingdom*

(Received 20 May 2014; published 26 November 2014; corrected 3 November 2020)

We study the statistics of the condition number $\kappa = \lambda_{\max}/\lambda_{\min}$ (the ratio between largest and smallest squared singular values) of $N \times M$ Gaussian random matrices. Using a Coulomb fluid technique, we derive analytically and for large N the cumulative $\mathcal{P}(\kappa < x)$ and tail-cumulative $\mathcal{P}(\kappa > x)$ distributions of κ . We find that these distributions decay as $\mathcal{P}(\kappa < x) \approx \exp[-\beta N^2 \Phi_-(x)]$ and $\mathcal{P}(\kappa > x) \approx \exp[-\beta N \Phi_+(x)]$, where β is the Dyson index of the ensemble. The left and right rate functions $\Phi_{\pm}(x)$ are independent of β and calculated exactly for any choice of the rectangularity parameter $\alpha = M/N - 1 > 0$. Interestingly, they show a weak nonanalytic behavior at their minimum (κ) (corresponding to the average condition number), a direct consequence of a phase transition in the associated Coulomb fluid problem. Matching the behavior of the rate functions around $\langle \kappa \rangle$, we determine exactly the scale of typical fluctuations $\sim O(N^{-2/3})$ and the tails of the limiting distribution of κ . The analytical results are in excellent agreement with numerical simulations.

DOI: [10.1103/PhysRevE.90.050103](https://doi.org/10.1103/PhysRevE.90.050103)

PACS number(s): 05.40.-a, 02.10.Yn, 02.50.Sk, 24.60.-k

Introduction. A classical task in numerical analysis is to find the solution \mathbf{x} of a linear system $A\mathbf{x} = \mathbf{y}$, where in the simplest setting A is a square $N \times N$ matrix and \mathbf{y} is a given column vector. The solution can be formally written as $\mathbf{x} = A^{-1}\mathbf{y}$ provided A is invertible. A very important issue for numerical stability is how a small change in the entries of \mathbf{y} or of A affects the solution \mathbf{x} ?

The system of equations above is said to be well (ill) conditioned if a small change in the coefficient matrix A or in the right-hand side \mathbf{y} results in a small (large) change in the solution vector \mathbf{x} . An ill-conditioned system produces a solution that cannot be trusted, as numerical inaccuracies in the inputs are amplified and propagated to the output [1].

The system of equations above is said to be well (ill) conditioned if a small change in the coefficient matrix A or in the right-hand side \mathbf{y} results in a small (large) change in the solution vector \mathbf{x} . An ill-conditioned system produces a solution that cannot be trusted, as numerical inaccuracies in the inputs are amplified and propagated to the output [1].

A standard indicator of the reliability of numerical solutions is the condition number (CN) $\kappa = \lambda_{\max}/\lambda_{\min} \geq 1$, where λ_{\min} and λ_{\max} are the smallest and largest squared singular values of A , i.e., the positive eigenvalues of AA^T (the square root $\sqrt{\kappa}$ of the CN is alternatively used frequently). The quantity $\ln_b \kappa$ is essentially a worst-case estimate of how many base- b digits are lost in solving numerically that linear system, which is singular if κ is infinite, ill conditioned if κ is too large, and well conditioned if κ is close to its minimum value 1.

Computing κ for a large coefficient matrix A in a fast and efficient way, however, can be as difficult a task as solving the original system in the first place [2]. To overcome this problem, Goldstine and von Neumann [3,4] proposed instead to study the generic features of κ associated with a random matrix A with normally distributed elements [5]. What is the typical (expected) CN for a system of size N ? What is a sensible estimate for the size of its fluctuations?

Apart from the various applications that the condition number has in numerical analysis [6], modern applications of a random condition number of more general (rectangular) matrices $N \times M$ include wireless communication systems

[7–11], spectrum sensing algorithms [12–14], convergence rate of iterative schemes [15], compressed sensing [16], finance [17], meteorology [18], and performance assessment of principal component analysis [19] among others. The statistics of $\sqrt{\kappa}$ was first computed by Edelman [20] for $2 \times M$ random Gaussian matrices, as well as the limiting distribution of $\sqrt{\kappa}/N$ for large $N \times N$ matrices. The rectangular case was recently considered in [21]. Different bounds for the tails were given in [22–24]. Exact formulas for the distribution of κ for finite N and M also exist in terms of cumbersome series of zonal polynomials [25,26] or an integral of a determinant [27], whose evaluation becomes impractical even for moderate matrix sizes. Approximate results for correlated noncentral Gaussian matrices can be found, e.g., in [28]. Other definitions for the CN also exist [5,29].

Unfortunately, almost nothing is known about the most dreaded (or welcomed) scenarios for applications, namely, the occurrence of atypical instances [30–33], where the CN is much larger (or smaller) than its expected value. In this Rapid Communication, by suitably adapting the Coulomb fluid method of statistical mechanics, we provide an analytical solution to this outstanding problem for large rectangular instances. We show that the large deviation statistics of the CN of Gaussian matrices, expressed in terms of elementary functions, has a rich and elegant structure. As a bonus, we also derive the scale of typical fluctuation of the CN around $\langle \kappa \rangle$ and the tails of its limiting distribution. Let us first summarize our setting and main results.

Summary of results. We consider rectangular $N \times M$ ($M > N$) matrices A with Gaussian distributed entries (real, complex, or quaternions, labeled by the Dyson index $\beta = 1, 2, 4$, respectively, or actually for general $\beta > 0$ as discussed in [34]). Forming the corresponding $N \times N$ covariance matrix $W = AA^T$,¹ which defines the Wishart ensemble [35], we define its rectangularity parameter $\alpha = M/N - 1 > 0$ and the

*On leave from Laboratoire de Physique Théorique et Modèles Statistiques, UMR No. 8626 associée au CNRS, Université Paris-Sud, Bâtiment 100, 91405 Orsay Cedex, France.

¹Here T stands for the transpose ($\beta = 1$), the Hermitian conjugate ($\beta = 2$), and the symplectic conjugate ($\beta = 4$).

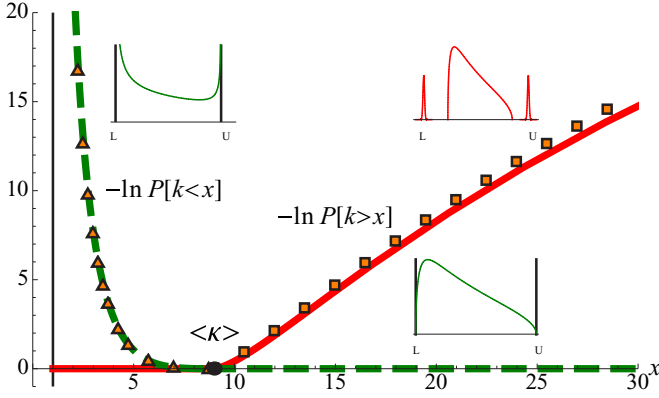


FIG. 1. (Color online) Plot of $-\ln \mathcal{P}(\kappa < x)$ [dashed green line, Eq. (1)] and $-\ln \mathcal{P}(\kappa > x)$ [solid red line, Eq. (2)], together with numerical simulations for the left and right branches [47]. The two rate functions $\beta N^2 \Phi_-(x)$ and $\beta N \Phi_+(x)$ freeze to the zero value upon crossing $\langle \kappa \rangle$. The insets describe the corresponding phases of the Coulomb fluid [active vs inactive barriers for $\Phi_-(x)$ and the pulling of individual extreme charges for $\Phi_+(x)$]. The Monte Carlo simulations have been performed with $N = 150$ for the left branch and $N = 70$ for the right one (for which we have used the method introduced in [46]). The value of M has been chosen in each case so that $\alpha = 3$. After the branches had been obtained numerically, an arbitrary value of N was chosen to produce a reasonable looking plot in which the two branches are visible.

CN $\kappa = \lambda_{\max}/\lambda_{\min} > 1$. Here λ_{\max} and λ_{\min} are the largest and smallest eigenvalues of W . We consider the cumulative $\mathcal{P}(\kappa < x)$ and tail-cumulative (also known as exceedance or survival function) $\mathcal{P}(\kappa > x)$ distributions of κ , when N and M are large and α is kept finite. Using a Coulomb fluid technique, we find that for large N both distributions obey large deviation laws, namely, they decay for large N as²

$$\mathcal{P}(\kappa < x) \approx \exp[-\beta N^2 \Phi_-(x)], \quad (1)$$

$$\mathcal{P}(\kappa > x) \approx \exp[-\beta N \Phi_+(x)]. \quad (2)$$

The left and right rate functions $\Phi_{\pm}(x)$ (depending parametrically on α , but not on β) are given in (11) and (13) and plotted in Fig. 1. Both functions are supported on $x \in (1, \infty)$ and have a minimum (zero) at $\langle \kappa \rangle = [(1 + \sqrt{1 + \alpha})/(1 - \sqrt{1 + \alpha})]^2 > 1$. Therefore, the corresponding density of κ is peaked around $\langle \kappa \rangle$, which is precisely its mean value for large N .³ Crossing $\langle \kappa \rangle$, both functions freeze to the zero value and around $\langle \kappa \rangle$ they have an interesting nonanalytic behavior, characterized by a third-order [for $\Phi_-(x)$] (see [36] for a recent review) and second-order [for $\Phi_+(x)$] discontinuity. Both these nonanalytic behaviors and the different scaling with N between (1) and (2) are direct consequences of phase transitions in an associated Coulomb fluid problem. The physics of the two branches, however, is entirely different,

²Here \approx stands for the logarithmic equivalence $\lim_{N \rightarrow \infty} -\ln \mathcal{P}(\kappa < x)/\beta N^2 = \Phi_-(x)$ and similarly for the tail-cumulative branch.

³The typical value $\langle \kappa \rangle$ for large N is just the ratio of the average $\langle \lambda_{\max} \rangle = (1 + \sqrt{1 + \alpha})^2$ and the average $\langle \lambda_{\min} \rangle = (1 - \sqrt{1 + \alpha})^2$.

as it is customary in this type of problems [36] (see below for details). Matching the behavior of the rate functions around $\langle \kappa \rangle$, we also determine exactly the size [$\sim O(N^{-2/3})$] of typical fluctuations of κ and the tails of its limiting distribution. We now begin by recalling some well-known facts about Wishart matrices.

Generalities. The probability density of the Wishart ensemble is given by

$$P_{\beta}(W) \propto e^{-\text{tr}W/2} (\det W)^{(\beta/2)(\alpha N + 1) - 1}, \quad (3)$$

where $\beta = 1, 2, 4$ is the Dyson index of the ensemble. A remarkable classical result is that the joint probability density (JPD) of the N (real and positive) eigenvalues can be written explicitly [by a formal diagonalization of Eq. (3)] and is given by [37,38]

$$P_{\beta}(\boldsymbol{\lambda}) = \frac{1}{Z_0} \exp\left(-\frac{1}{2} \sum_{i=1}^N \lambda_i\right) \prod_{i=1}^N \lambda_i^{(\beta/2)(\alpha N + 1) - 1} \times \prod_{i < j} |\lambda_i - \lambda_j|^{\beta}, \quad (4)$$

where Z_0 is a normalization constant. Note that this JPD is for the ordered eigenvalues and so it is normalized in the Weyl chamber $0 < \lambda_1 < \lambda_2 < \dots < \infty$. Balancing the first and third terms in (4), it is quite easy to estimate that the typical scale of an eigenvalue is $\sim O(N)$. Thus, after rescaling $\lambda_i \rightarrow \beta N \lambda_i$, the JPD (4) can be rewritten in the form $P_{\beta}(\boldsymbol{\lambda}) \propto \exp(-\beta N^2 E[\{\boldsymbol{\lambda}\}])$, where the $O(1)$ energy is

$$E[\{\boldsymbol{\lambda}\}] = \frac{1}{2N} \sum_{j=1}^N \lambda_j - \frac{\alpha}{2N} \sum_{j=1}^N \ln \lambda_j - \frac{1}{2N^2} \sum_{j \neq k} \ln |\lambda_j - \lambda_k|. \quad (5)$$

Written in this form, the JPD (4) is the Gibbs-Boltzmann canonical weight of a two-dimensional fluid of charged particles, confined on the semi-infinite (positive) line and in equilibrium at inverse temperature β under competing interactions: the external linear-logarithmic potential in (5) drives the charges towards its minimum, while the third term (representing an all-to-all repulsive interaction of the Coulomb type in two dimensions) spreads them apart. This thermodynamical analogy, originally pioneered by Dyson [39], has been employed in several different contexts [36,40–46].

The average spectral density of the Wishart model $\rho(\lambda) = N^{-1} \sum_{i=1}^N \langle \delta(\lambda - \lambda_i) \rangle$ [where $\langle \dots \rangle$ denotes averaging with respect to the JPD (4)] is expected for large N to have the scaling form $\rho(\lambda) = N^{-1} \rho_{\text{MP}}(\lambda/N)$, where the function $\rho_{\text{MP}}(x) = \frac{1}{2\pi x} \sqrt{(x - z_-)(z_+ - x)}$ is the celebrated Marčenko-Pastur (MP) law on the compact support (for $\alpha > 0$) $x \in [z_-, z_+]$ with $z_{\pm} = (1 \pm \sqrt{\alpha + 1})^2$. This MP law is a particular case of the general solution (10) of the integral equation (9) below (see Fig. 2, top) when the two barriers L and U are ineffective ($L \leq z_-$ and $U \geq z_+$). We start now by considering the cumulative distribution of the CN first and get to the tail-cumulative afterward.

Cumulative distribution. The cumulative distribution $\mathcal{P}(\kappa < x)$ of the CN κ (depending parametrically on β and

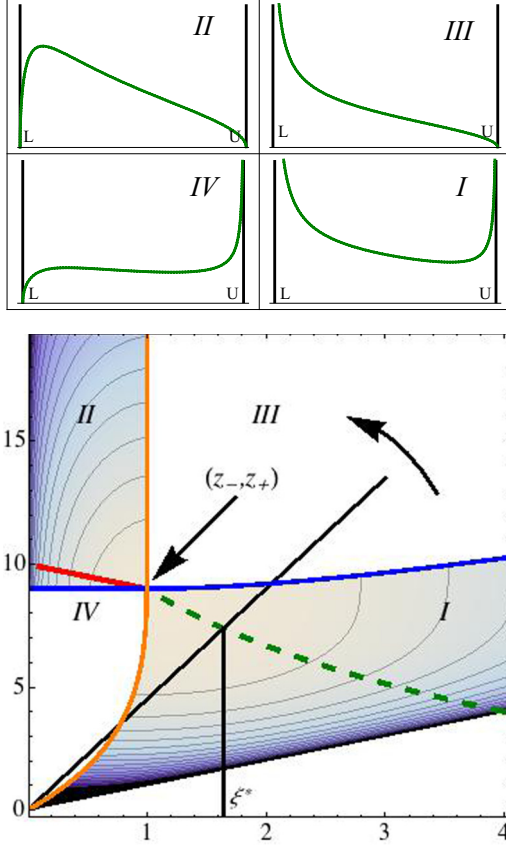


FIG. 2. (Color online) Shown on the top are the four phases of the fluid: region I, the two barriers compress effectively the fluid; region II, MP law, where the barriers do not affect the fluid; and regions III and IV, only the lower or the upper barrier is active, respectively (this scenario is not realized in our CN setting). The analytical expressions in regions III and IV were first derived in [42,44], respectively. Shown on the bottom are the regions in the (L, U) plane where the density equation (10) has different shapes, according to the top panels, for $\alpha = 3$. We plot level curves of the action (8) $S[\rho^*, C; L, U]$ (I) and energy difference $\Delta e(L, U)$ (see in [47]) (IV). On the dashed green and solid red extremal lines, the action and the energy difference are minimal, respectively. The abscissas ξ^* (solution of the saddle-point equations in the two cases) are given by the intersection of the straight line $U = xL$ (solid black, with the left arrow pointing in the direction of increasing slope x) with such extremal lines. In addition, the solid orange line corresponds to the condition $x_-(L, U) = L$ along which the lower barrier is ineffective (and the upper is effective), while the solid blue line corresponds to the condition $x_+(L, U) = U$ along which the upper barrier is ineffective (and the lower is effective).

$\alpha = M/N - 1 > 0$) can be written as [27,47]

$$\mathcal{P}(\kappa < x) = \frac{1}{(N-1)!} \int_0^\infty d\lambda_1 \left[\int \cdots \int_{\lambda_1}^{x\lambda_1} \prod_{j=2}^N d\lambda_j P_\beta(\lambda) \right]. \quad (6)$$

The goal is to evaluate this multiple integral for large N by the Coulomb fluid method. The first step is to rewrite the JPD (4) in the Gibbs-Boltzmann form described above. Here $N - 1$ fluid particles are, however, not free to spread on the whole positive

line, but instead constrained to exist within the box $[\lambda_1, x\lambda_1]$, where λ_1 is the (free) position of the leftmost particle.

The second step consists of a coarse-graining procedure, where one introduces a normalized density of particles $\rho(\lambda) = (N-1)^{-1} \sum_{i=2}^N \delta(\lambda - \lambda_i)$ for the $N - 1$ particles λ_i ($i \neq 1$) existing inside the box. Using the replacement rule $\sum_{i>1} g(\lambda_i) = (N-1) \int d\lambda \rho(\lambda) g(\lambda)$, we can convert the energy function $E[\{\lambda\}]$ into a continuous action S (depending on ρ and parametrically on the location of the leftmost particle λ_1 and x). The multiple integration (6) is therefore interpreted as the canonical partition function of the associated Coulomb fluid, where the sum over all microscopic configurations of $\{\lambda\}$ compatible with the normalized density ρ amounts to a functional integration over ρ and a standard integration over λ_1 . Eventually, these resulting integrals are evaluated using the saddle-point method. Performing these steps, we get

$$\mathcal{P}(\kappa < x) \propto \int_0^\infty d\xi \int \mathcal{D}[\rho, C] e^{-\beta N^2 S[\rho, C; \xi, x\xi]}, \quad (7)$$

where we renamed $\lambda_1 \rightarrow \xi$ for later convenience and the action of this fluid (confined between the lower L and upper U barriers of the box) is

$$S[\rho, C; L, U] = \int_L^U d\lambda \rho(\lambda) V(\lambda) + C - \frac{1}{2} \iint_L^U d\lambda d\lambda' \rho(\lambda) \rho(\lambda') \ln |\lambda - \lambda'|. \quad (8)$$

Here $V(\lambda) = (\lambda - \alpha \ln \lambda)/2 - C$ and C is a Lagrange multiplier enforcing normalization of ρ . Equation (8) is easily identified as the continuous version of the energy equation (5), where we have neglected subleading $O(N)$ contributions [47]. The action for a Coulomb fluid constrained between two barriers in the presence of a quadratic confining potential instead was first derived in [40].

Evaluating the functional integral in (7) by the saddle-point method $\frac{\delta S}{\delta \rho} \Big|_{\rho=\rho^*} = 0$, we get the saddle-point equation

$$V(\lambda) = \int_L^U d\lambda' \rho^*(\lambda') \ln |\lambda - \lambda'|, \quad (9)$$

where the solution $\rho^*(\lambda)$ is just the equilibrium density of the Coulomb fluid constrained to exist within the box $[L, U]$. Clearly, if we release the barriers L and U we expect to recover the unconstrained MP law $\rho^*(\lambda) \rightarrow \rho_{\text{MP}}(\lambda)$.

Solving this integral equation for a normalized ρ^* between two barriers at L and U is one of the main technical challenges that we managed to overcome. Skipping details [47], we find that the general solution of (9) is [48]

$$\rho^*(\lambda) = \frac{[x_+(L, U) - \lambda][\lambda - x_-(L, U)]}{2\pi \lambda \sqrt{(U - \lambda)(\lambda - L)}} \mathbb{1}_{[L, U]}(\lambda), \quad (10)$$

where $x_+(L, U) \geq U > L \geq x_-(L, U)$, $x_\pm(L, U)$ are the roots of $x^2 - x(\frac{L+U}{2} + \alpha + 2) + \alpha\sqrt{LU} = 0$, and $\mathbb{1}_{[a, b]}(x)$ is the indicator function, that is, $\mathbb{1}_{[a, b]}(x) = 1$ if $x \in [a, b]$ and 0 otherwise.

What does this density look like for given values of L and U ? Four different shapes (phases of the fluid) are possible [47] for $\alpha > 0$, which are plotted in Fig. 2 (top). For example, setting $(L, U) = (z_-, z_+)$, the corresponding density (10) is

the MP law $\rho^*(x) = \rho_{\text{MP}}(x)$ (phase II). This critical MP point, which is marked in Fig. 2 (bottom), separates region II, where the barriers are ineffective ($L < z_-$ and $U > z_+$) and the equilibrium density is again just $\rho_{\text{MP}}(x)$, from region I (where the barriers are instead effective in compressing the MP sea).

Once we have evaluated the functional integral by the saddle-point method [which implies inserting the density (10) in the action (8)] we set $L = \xi$ and $U = x\xi$ and evaluate the remaining ξ integral again by the saddle-point method. This yields an optimal value ξ^* as the solution of $\frac{d}{d\xi} S[\rho^*, C; \xi, x\xi]_{\xi=\xi^*} = 0$. This value $\xi^*(x)$ is marked in Fig. 2 (bottom) as the intersection between the straight line $U = xL$ of varying slope $x > 1$ and the dashed green line on which the action $S[\rho^*, C; L, U]$ is minimal.

The final result reads $\mathcal{P}(\kappa < x) \approx e^{-\beta N^2 \Phi_-(x)}$, where the $O(N^2)$ decay is traced back to the high-energy cost in compressing the whole sea of strongly correlated particles. Here $\Phi_-(x) = S[\rho^*, C; \xi^*, x\xi^*] - S[\rho_{\text{MP}}, C; z_-, z_+]$, where the second term comes from the normalization factor and needs to be subtracted. We eventually obtain

$$\Phi_-(x) = \frac{1}{8} [f_1^{(\alpha)}(1 + \sqrt{x}) + \ln f_2^{(\alpha)}(1 + \sqrt{x})] \mathbb{1}_{(1, \langle \kappa \rangle)}(x), \quad (11)$$

where $f_{1,2}^{(\alpha)}(\omega)$ are elementary functions listed in [47]. The rate function $\Phi_-(x)$ thus freezes to the value 0 as x increases up to the critical value $\langle \kappa \rangle$ [implying $\xi^*(\langle \kappa \rangle) \rightarrow z_-$]. Beyond this limit, the barriers are no longer effective and new physical insights are needed to tackle the tail-cumulative regime (see the next section). The limits are $\Phi_-(x \rightarrow \langle \kappa \rangle^-) \sim K(\alpha)(\langle \kappa \rangle - x)^3$ and $\Phi_-(x \rightarrow 1^+) \sim (-1/2) \ln(x - 1)$, where $K(\alpha) = -(-1 + \sqrt{1 + \alpha})^8 / [96\sqrt{1 + \alpha}(1 + \sqrt{1 + \alpha})^4]$. This implies a third-order discontinuity across $\langle \kappa \rangle$ as anticipated. Also, close to 1, the density of κ has the power-law tail $\mathcal{P}(\kappa = 1 + \epsilon) \sim \epsilon^{\beta N^2/2}$ to leading order in N for $\epsilon \rightarrow 0^+$. Although formally valid only for $\alpha > 0$, it turns out that in the limit $\alpha \rightarrow 0$ (square Gaussian matrices, where the scaling with N is different) the rate function (11) is still well behaved and we recover Edelman's result [20] to leading order in N [47]. We now turn to the tail-cumulative distribution (the right branch in Fig. 1).

Tail-cumulative distribution. Contrary to the previous case, the tail-cumulative distribution $\mathcal{P}(\kappa > x)$ does not admit a multiple-integral representation of the type (6), which could be mapped to the physics of a fluid trapped between two hard barriers. The starting point of the calculation is again the energy function (5) though. The Coulomb fluid physics suggests that atypically large values of the CN $\kappa = \lambda_{\text{max}}/\lambda_{\text{min}}$ are obtained when the rightmost and leftmost particles are pulled away from the MP sea in opposite directions [$\lambda_{\text{max}} - \lambda_{\text{min}} \sim O(N)$], a procedure that is energetically not able to generate macroscopic rearrangements within the MP sea. This elegant energetic argument was first introduced in [43]. Following this physical picture, the right rate function $\Phi_+(x)$ is determined by the $O(N)$ energy cost $\Delta E(L, U)$ in pinning the leftmost and rightmost charges at L and U , well outside the unperturbed MP sea in between (see the red inset in Fig. 1). The level curves of the $O(1)$, $\Delta e(L, U) := \Delta E(L, U)/\beta N$, are depicted in region II of Fig. 2, together with the extremal line

(solid red line) where it attains its minimum value. Setting now $L = \xi$ and $U = \xi x$, the energetically most favored position ξ^* for the leftmost outlier will be determined again by the intersection point of that extremal line and the straight line $U = xL$.

Skipping details [47], this change in energy can be written for large N as

$$\Delta e(\xi, \xi x) = \frac{(\xi - z_-) + (\xi x - z_+)}{2} - \frac{\alpha}{2} \ln \frac{\xi^2 x}{z_- z_+} - \int_{z_-}^{z_+} d\eta \rho_{\text{MP}}(\eta) \ln \left| \frac{(\xi - \eta)(\eta - \xi x)}{(z_- - \eta)(\eta - z_+)} \right|. \quad (12)$$

The probability of this pinned configuration of eigenvalues (yielding a CN κ exactly equal to x) is proportional to $\exp[-\beta N \Delta e(\xi, \xi x)]$. Finding the optimal position ξ^* for the leftmost particle by minimizing (12) with respect to ξ , we eventually obtain $\mathcal{P}(\kappa > x) \approx \exp[-\beta N \Phi_+(x)]$, where $\Phi_+(x) = \Delta e[\xi^*(x), \xi^*(x)x]$ is given by⁴

$$\Phi_+(x) = \ln\{[g^{(\alpha)}(x)]^{\alpha/2} [h^{(\alpha)}(x)]^{2(2+\alpha)}\} \mathbb{1}_{(\langle \kappa \rangle, \infty)}(x). \quad (13)$$

The functions $g^{(\alpha)}(x)$ and $h^{(\alpha)}(x)$ have lengthy but explicit expressions in terms of elementary functions [47]. The rate function $\Phi_+(x)$ again freezes to the value 0 as x decreases down to the critical value $\langle \kappa \rangle$ [implying $\xi^*(\langle \kappa \rangle) \rightarrow z_-$], where the pinned outliers reconnect with the MP sea. The limits are $\Phi_+(x \rightarrow \langle \kappa \rangle^+) \sim J(\alpha)(x - \langle \kappa \rangle)^{3/2}$ and $\Phi_+(x \rightarrow \infty) \sim (\alpha/2) \ln x$, where $J(\alpha) = \sqrt{2}^4 \sqrt{\alpha + 1} (\sqrt{\alpha + 1} - 1)^4 / [3\sqrt{\alpha + 2} (\sqrt{\alpha + 1} + 1)^2]$. This implies a discontinuity in the second derivative across $\langle \kappa \rangle$ as anticipated. Also, at infinity the density of κ therefore decays as a power law $\mathcal{P}(\kappa = x) \sim x^{-\alpha\beta N/2}$ to leading order in N for $x \rightarrow \infty$.

Conclusion. In summary, we have computed analytically for large N the cumulative and tail-cumulative distributions of the CN of rectangular $N \times M$ Gaussian random matrices. The rate functions (11) and (13), describing the probability of sampling a random Gaussian matrix with an atypically large (or small) CN, display a nonanalytic behavior that is a direct consequence of a very rich thermodynamics of the associated Coulomb fluid.

Matching the behavior of the rate functions close to their minimum $\langle \kappa \rangle$, we deduce that typical fluctuations of κ around $\langle \kappa \rangle$ should occur on a scale of $O(N^{-2/3})$ and setting $\chi = f(\alpha) N^{2/3} (\kappa - \langle \kappa \rangle)$, with $f(\alpha) = 2^{1/3} (1 + \alpha)^{1/6} (-1 + \sqrt{1 + \alpha})^{8/3} / (1 + \sqrt{1 + \alpha})^{4/3}$, the scaled random variable χ has an N - and α -independent distribution $\mathcal{P}(\chi < x) = \mathcal{F}_\beta(x)$ with tails $\sim \exp(-\beta|x|^3)$ for $x \rightarrow -\infty$ and $\sim \exp(-\beta x^{3/2})$ for $x \rightarrow \infty$. The scaling is in agreement with a recent result [21], valid only for $M \gg N^3$. Our analytical results have been numerically checked with excellent agreement [47].

Acknowledgments. This work is supported by ‘‘Investissements d’Avenir’’ LabEx PALM (ANR-10-LABX-

⁴Note that this energetic argument gives (strictly speaking) the density of κ , $\mathcal{P}(\kappa = x)$, and not its tail-cumulative distribution $\mathcal{P}(\kappa > x)$. However, the large- N decay of the two is the same to leading order.

0039-PALM) [P.V.]. We thank G. Schehr and F. D. Cunden for helpful discussions. I.P.C. acknowledges hospitality by

the LPTMS (Université Paris–Sud) where this work was completed.

-
- [1] S. Smale, *Bull. Am. Math. Soc.* **13**, 87 (1985).
- [2] H. Avron, A. Druinsky, and S. Toledo, [arXiv:1301.1107](https://arxiv.org/abs/1301.1107).
- [3] J. von Neumann and H. H. Goldstine, *Bull. Amer. Math. Soc.* **53**, 1021 (1947).
- [4] H. H. Goldstine and J. von Neumann, *Am. Math. Soc. Proc.* **2**, 188 (1951).
- [5] J. W. Demmel, *Math. Comput.* **50**, 449 (1988).
- [6] L. R. Scott, *Numerical Analysis* (Princeton University Press, Princeton, 2011).
- [7] V. Erceg, P. Soma, D. S. Baum, and A. J. Paulraj, *Proceedings of the IEEE International Conference on Communications* (IEEE, Piscataway, 2002), Vol. 1, pp. 396–400.
- [8] M. D. Batarieri *et al.*, *Proceedings of the IEEE Conference on Vehicular Technology* (IEEE, Piscataway, 2002), pp. 26–30.
- [9] H. Artes, D. Seethaler, and F. Hlawatsch, *IEEE Trans. Signal Process.* **51**, 2808 (2003).
- [10] D. Wübben, R. Böhnke, V. Kühn, and K. D. Kammeyer, *Proceedings of the ITG Workshop on Smart Antennas* (IEEE, Piscataway, 2004), pp. 106–113.
- [11] J. Maurer, G. Matz, and D. Seethaler, *Proceedings of the IEEE International Conference on Acoustics, Speech and Signal Processing* (IEEE, Piscataway, 2007), Vol. 3, pp. 61–64.
- [12] Y. Zeng and Y.-C. Liang, *IEEE Trans. Commun.* **57**, 1784 (2009).
- [13] F. Penna, R. Garello, and M. Spirito, *IEEE Commun. Lett.* **13**, 507 (2009).
- [14] L. S. Cardoso, M. Debbah, P. Bianchi, and J. Najim, *Proceedings of the IEEE International Symposium on Wireless Pervasive Computing* (IEEE, Piscataway, 2008), pp. 334–338.
- [15] G. Strang, *Linear Algebra and its Applications*, 3rd ed. (Harcourt Brace Jovanovich, San Diego, 1988).
- [16] H. Rauhut, *Theoretical Foundations and Numerical Methods for Sparse Recovery* (de Gruyter, Berlin, 2010), pp. 1–92.
- [17] A. Binder and M. Aichinger, *A Workout in Computational Finance* (Wiley, New York, 2013).
- [18] M. Piringer, M. Hrad, S. Stenzel, and M. Huber-Humer, Proceedings of 15th Conference on Harmonisation within Atmospheric Dispersion Modelling for Regulatory Purposes, available at <http://www.harmonisation.org/conferences/Madrid/15harmo.asp>.
- [19] *Computational Intelligence in Medical Informatics*, edited by A. Kelemen, A. Abraham, and Y. Liang, Studies in Computational Intelligence Vol. 85 (Springer, Berlin, 2008).
- [20] A. Edelman, *SIAM J. Matrix Anal. Appl.* **9**, 543 (1988).
- [21] T. Jiang and D. Li, *J. Theor. Probab.*, doi:10.1007/s10959-013-0519-7.
- [22] A. Edelman and B. D. Sutton, *SIAM J. Matrix Anal. Appl.* **27**, 547 (2005).
- [23] Z. Chen and J. J. Dongarra, *SIAM J. Matrix Anal. Appl.* **27**, 603 (2005).
- [24] J.-M. Azaïs and M. Wschebor, *SIAM J. Matrix Anal. Appl.* **26**, 426 (2005).
- [25] W. Anderson and M. T. Wells, *SIAM J. Matrix Anal. Appl.* **31**, 1125 (2009).
- [26] T. Ratnarajah, R. Vaillancourt, and M. Alvo, *SIAM J. Matrix Anal. Appl.* **26**, 441 (2005).
- [27] M. Matthaiou, M. R. McKay, P. J. Smith, and J. A. Nossek, *IEEE Trans. Commun.* **58**, 1705 (2010).
- [28] L. Wei and O. Tirkkonen, *Proceedings of the IEEE International Conference on Communications* (IEEE, Piscataway, 2011), pp. 1–5.
- [29] A. Edelman, *Math. Comput.* **58**, 185 (1992).
- [30] R. A. Fisher and L. H. C. Tippett, *Proc. Cambridge Philos. Soc.* **24**, 180 (1928).
- [31] B. Gnedenko, *Ann. Math.* **44**, 423 (1943).
- [32] W. Weibull, *J. Appl. Mech. Trans. ASME* **18**, 293 (1951).
- [33] E. J. Gumbel, *Statistics of Extremes* (Dover, New York, 1958).
- [34] I. Dumitriu and A. Edelman, *J. Math. Phys.* **43**, 5830 (2002).
- [35] J. Wishart, *Biometrika* **20A**, 32 (1928).
- [36] S. N. Majumdar and G. Schehr, *J. Stat. Mech.* (2014) P01012.
- [37] R. A. Fisher, *Ann. Eugenics* **9**, 238 (1939).
- [38] P. L. Hsu, *Ann. Eugenics* **9**, 250 (1939).
- [39] F. J. Dyson, *J. Math. Phys.* **3**, 140 (1962); **3**, 157 (1962); **3**, 166 (1962).
- [40] D. S. Dean and S. N. Majumdar, *Phys. Rev. E* **77**, 041108 (2008).
- [41] D. S. Dean and S. N. Majumdar, *Phys. Rev. Lett.* **97**, 160201 (2006).
- [42] P. Vivo, S. N. Majumdar, and O. Bohigas, *J. Phys. A: Math. Theor.* **40**, 4317 (2007).
- [43] S. N. Majumdar and M. Vergassola, *Phys. Rev. Lett.* **102**, 060601 (2009).
- [44] E. Katzav and I. Pérez Castillo, *Phys. Rev. E* **82**, 040104(R) (2010).
- [45] C. Texier and S. N. Majumdar, *Phys. Rev. Lett.* **110**, 250602 (2013).
- [46] N. Saito, Y. Iba, and K. Hukushima, *Phys. Rev. E* **82**, 031142 (2010).
- [47] See Supplemental Material at <http://link.aps.org/supplemental/10.1103/PhysRevE.90.050103> for details in the derivations as well as explanation on the Monte Carlo methods.
- [48] F. G. Tricomi, *Integral Equations* (Interscience, London, 1957).